

# Performance of the CMS tracking detectors from the 2009 LHC run

**Keith A. Ulmer, on behalf of the CMS collaboration**

University of Colorado

**Abstract.** The 2009 run provided the first proton-proton collisions from the Large Hadron Collider (LHC) at center of mass energies of 900 GeV and 2.36 TeV. The Compact Muon Solenoid (CMS) experiment has recorded a large sample of minimum bias events from these collisions. We present results from the all silicon tracking detectors from this run. The performance of the tracker and track reconstruction algorithms are considered including signal-to-noise, efficiencies and comparisons to simulation for track parameter and resonance reconstruction performance.

## 1. Introduction

The first collisions at CMS were recorded in December 2009 at energies of  $\sqrt{s} = 900$  GeV and 2.36 TeV. The reconstructed tracks in this data have been studied extensively to commission the tracking detectors and to reconstruct basic physics objects as a demonstration of the performance. In these proceedings, we describe the results of some of these studies.

The CMS tracker is an all silicon design consisting of two main detectors: a silicon pixel detector, covering the region from  $\approx 4$  cm to  $\approx 11$  cm in radius, and  $\approx 27$  cm on either side of the collision point along the LHC beam axis, and a silicon strip detector, covering the region from  $\approx 25$  cm to  $\approx 110$  cm in radius, and  $\approx 280$  cm on either side of the collision point along the LHC beam axis. The pixel detector has 66 million channels covering an active surface area of about  $1 \text{ m}^2$  that provide precise three-dimensional information about charged track positions. The strip detector has 9.3 million channels covering an area of  $198 \text{ m}^2$ . Both are arranged in a pattern of concentric cylinders to cover the central region and discs to cover the forward regions. Additional details can be found in [1].

## 2. Tracker Performance

The 2009 run was used to evaluate the performance of the tracker and to perform various calibrations needed to operate with the best performance and highest efficiency possible in future runs. A fraction of 98.4% of the pixel channels were operational. The remaining 1.6% of inoperable channels was due mainly to channels with a slow signal rise time, which may be recoverable for future running. The strip detector operated with 97.2% of its channels functioning well, with most of the inoperable channels due to voltage supply shorts or leaks in the cooling system. The system is built with large redundancy and the effect of the missing channels on track reconstruction performance is minimal.

The 2009 LHC collisions provided the first opportunity to record tracks from particles produced in time with the LHC clock. The pixel detector readout system uses the 40 MHz

LHC clock as input. Signals from the CMS trigger system must arrive at the correct time within the 25 ns clock cycle to associate the correct bunch crossing time stamp with any signal above the readout threshold. An optimally phased clock signal will maximize the number of pixels observed in the recorded clusters. The overall trigger timing was adjusted by varying the clock phase until the average cluster size was maximized. A finer module-by-module adjustment of the clock phase will be performed when higher trigger rates become available. A similar timing scan was performed for the strip detector and the delay with the largest mean collected charge per cluster was chosen for future running. The timing for the strip detector is not as sensitive as for the pixels due to the wider pulse shape.

After optimizing the timing delays, the performance of the pixel and strip detectors was evaluated. The left plot of Figure 1 shows the distribution of collected charge per cluster recorded by the barrel pixel detectors compared to simulation, where in both data and simulation the charge is normalized to the track path length through the silicon. The peak of the charge collection shows good agreement with simulation, though the data distribution is somewhat more broad than simulation.

The strip detector signal over noise was measured for each module where the signal was taken from clusters reconstructed in tracks, and noise was evaluated in calibration runs. The S/N varies with the thickness and length of the sensor. A representative plot is shown for inner strip barrel sensors (TIB) in the right plot of Figure 1, where the characteristic Landau distribution of collected charge is observed. The most probable values of the S/N values range from 18.8 to 24.5 depending on the sensor thickness and are in good agreement with simulation. The efficiency of the strip detector sensors was measured by using reconstructed tracks to search for the presence of a recorded hit on modules known to have been traversed by the track. For operational modules the efficiency is measured to be in excess of 99.9%.

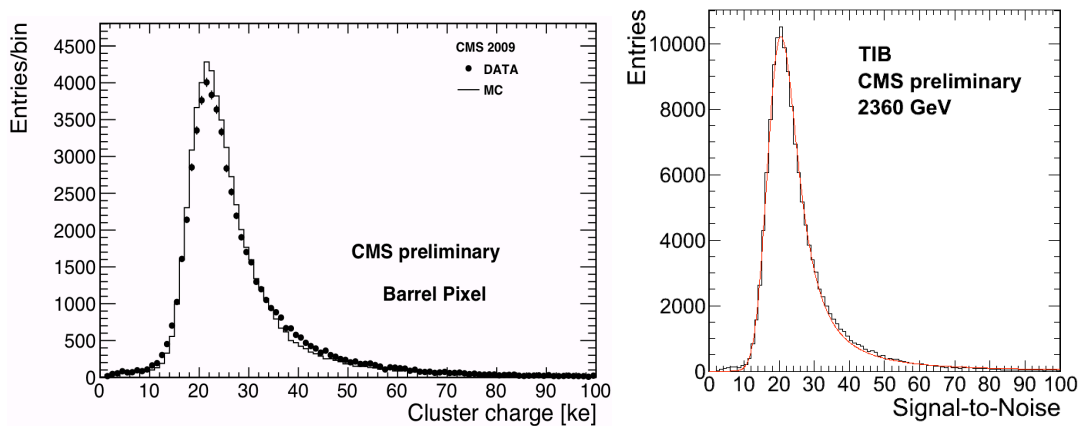


**Figure 1.** Charge per cluster in the pixel barrel layers compared to simulation (left) and strip signal/noise ratio for clusters on tracks in inner barrel layers (right).

### 3. Track Reconstruction Performance

The standard track reconstruction at CMS is performed by the combinatorial track finder [2]. Tracks are seeded from either triplets of hits in the tracker or pairs of hits with an additional constraint from the beamspot or a pixel vertex, yielding an initial estimate of the trajectory, including its uncertainty. The seed is then propagated outward in a search for compatible hits. As hits are found, they are added to the trajectory and the track parameters and uncertainties

are updated. This search continues until either the boundary of the tracker is reached or no more compatible hits can be found.

Reconstructed tracks are filtered to remove tracks that are likely fakes and to provide a means of quantifying the quality of the remaining tracks. The filtering uses information on the number of hits, the normalized  $\chi^2$  of the track, and the compatibility of the track originating from a pixel vertex. Tracks that pass the tightest selection are labeled *highPurity* [3]. The *highPurity* tracks are selected, with additional requirements of  $|d_z| < 10\sigma_z$  (where  $\sigma_z$  is the combined track and primary vertex uncertainty) and  $\sigma_{p_T}/p_T < 10\%$  to compare the data and simulation. The left plot of Figure 2 shows the results of this comparison for the track transverse momentum, where the distribution has been normalized to the number of reconstructed tracks in the data. As with  $p_T$ , there is general agreement between the data and simulation in the shape of all variables.

The reconstruction of the primary interaction vertex in the event starts from the track collection. After filtering the tracks, they are clustered in  $z$  and the cluster is fit with an adaptive vertex fit, where tracks in the vertex are assigned a weight between 0 and 1 based on their proximity to the common vertex. The primary vertex resolution is strongly dependant on the number of tracks used in fitting the vertex. To measure the resolution, the tracks in an event are split into two different sets and used to independently fit the primary vertex. The distribution of the difference in the fitted vertex positions can then be used to extract the resolution by fitting a Gaussian to the distribution and dividing  $\sigma$  by  $\sqrt{2}$ . The right plot of Figure 2 shows the  $x$  resolution of the primary vertex position as a function of the number of tracks in the vertex. Good agreement between data and simulation is observed.

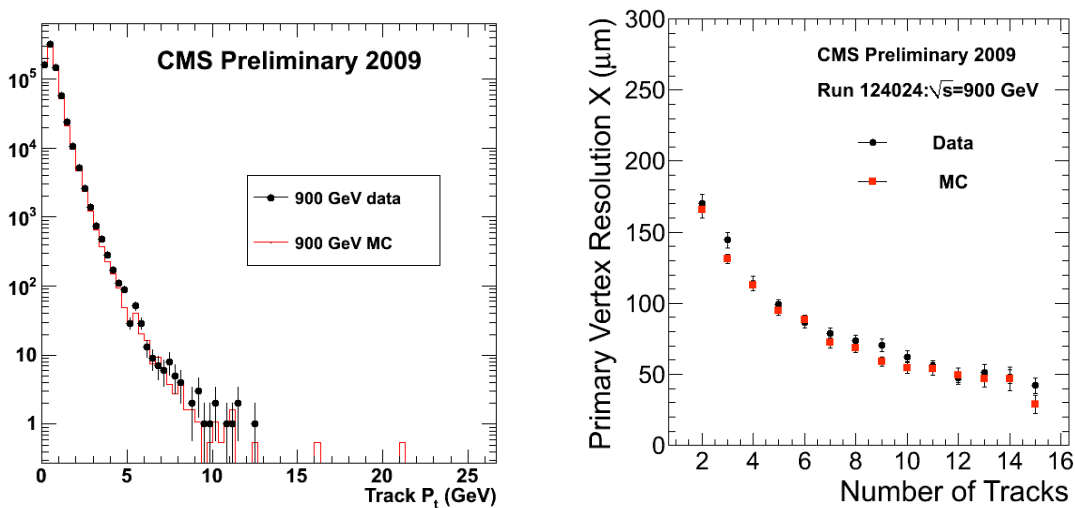


**Figure 2.** Track transverse momentum distribution compared to simulation (left), and primary vertex resolution vs number of tracks compared to simulation (right).

With a collection of well reconstructed tracks, a number of resonances can be reconstructed from our data sample. Long-lived strange particles,  $K_S^0$  and  $\Lambda^0$ , were reconstructed in their decays to two charged particles,  $\pi^+\pi^-$  and  $p\pi^-$ , respectively.<sup>1</sup> The reconstruction is performed by finding oppositely charged tracks which are detached from the primary vertex and form a good vertex with an appropriate invariant mass. The tracks are required to have at least 6 hits, a normalized  $\chi^2 < 5$  and a transverse impact parameter with respect to the beamspot

<sup>1</sup> Charge conjugate decays are implied throughout.

greater than  $0.5\sigma$ . The reconstructed decay vertex must have a  $\chi^2$  less than 7 and a transverse separation from the beamspot greater than  $15\sigma$ . The resulting distributions show clear peaks for these resonances as shown in Figure 3.

With the sample of  $\Lambda^0$  particles, the cascade decay  $\Xi^- \rightarrow \Lambda^0 \pi^-$  can also be reconstructed. The  $\pi^-$  from the  $\Xi^-$  will also be detached from the primary vertex due to the  $\Xi^-$  lifetime.  $\Lambda^0$  candidates are reconstructed as described above, except with a looser transverse significance cut of 10, and combined with charged tracks with the same sign as the pion in the  $\Lambda^0$  decay. The  $\Lambda^0 \pi^-$  fit applies a  $\Lambda^0$  mass constraint and the vertex is required to have a fit probability greater than 1%. All three tracks involved in the decay were required to have at least 6 valid hits and a 3D impact parameter with respect to the primary vertex greater than  $3\sigma$ . The resulting mass peak is shown in Figure 3.

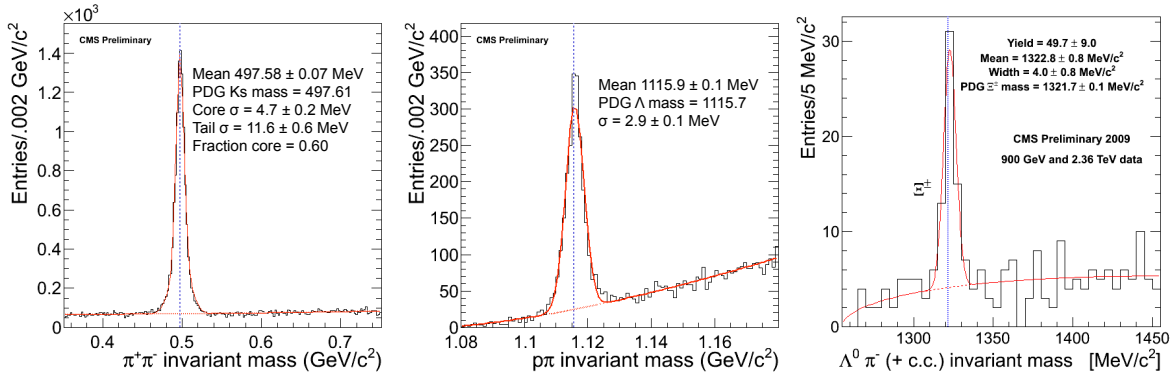


**Figure 3.** Invariant mass distributions from  $\pi^+\pi^-$ ,  $p\pi^-$  and  $\Lambda^0\pi^-$  combinations (left to right).

#### 4. Conclusion

The performance of the CMS tracker has been studied using the collision data provided by the LHC in the 2009 run. The tracker has been shown to perform well and is in good agreement with the expectations from simulation. The track reconstruction algorithm has also been shown to robustly reconstruct charged tracks and allow for the reconstruction of the  $K_S^0$ ,  $\Lambda^0$  and  $\Xi^-$  resonances.

- [1] The CMS Collaboration, JINST **0803**, S08004 (2008).
- [2] Adam, W., Mangano, B., Speer, Th. and Todorov, T., CMS Note **2006/041**, [http://cms.cern.ch/iCMS/jsp/openfile.jsp?type=NOTE&year=2006&files=NOTE2006\\_041.pdf](http://cms.cern.ch/iCMS/jsp/openfile.jsp?type=NOTE&year=2006&files=NOTE2006_041.pdf) (2006).
- [3] The CMS Collaboration, CMS Physics Analysis Summary **TRK-10-001**, <http://cms-physics.web.cern.ch/cms-physics/public/TRK-10-001-pas.pdf> (2010).